INSTITUTE

for

FLUID DYNAMICS

and

APPLIED MATHEMATICS

Technical Note BN-757 January 1973

ION OPTICAL DESIGN WITH APPLICATIONS TO A SOLAR WIND MASS SPECTROMETER*

by

Michael Coplan

UNIVERSITY OF MARYLAND
College Park

ION OPTICAL DESIGN WITH APPLICATIONS TO A SOLAR WIND MASS SPECTROMETER*

by

Michael Coplan
University of Maryland
College Park, Maryland
20742

*This work was supported by NASA grant NGR 21-002~~0~~291

TABLE OF CONTENTS

ION OPTICAL DESIGN WITH APPLICATIONS TO A SOLAR WIND MASS SPECTROMETER*

I. Introduction

Much of the material on the subject of ion optics is derived from electron optics where the energies involved are often upward of several kilovolts. When dealing with charged particle transport below a few kilovolts, design methods and considerations are generally less well known and much of the information is in journal articles. General texts describing exactly how to design charged particle beam tramsport systems at lower energies are lacking.

II. General Relations

A. Index of Refraction

1. Snell's law and light optics.

$$n \sin \Theta = n' \sin \Theta' \qquad (1)$$

where n and n' are the indices of refraction on two sides of a plane boundary and Θ and Θ' are the angles of incidence and refraction of a light ray as measured with respect to the normal to the boundary. For the case of charged particle optics, consider a potential boundary separating two regions of electrical potential V and V'. In a manner analogous to light optics the tangential component of velocity of the particle will be unchanged at the boundary. If v and v' are the velocities of the particle on the two sides of the boundary

*Work supported by NASA grant NGR 21-0020291

$$v \sin \Theta = v' \sin \Theta' \ .$$

Setting the kinetic energy of the particle equal to the product of its charge and the electrical potential

$$1/2\ mv^2 = eV \ , \ 1/2\ mv'^2 = eV' \tag{3a}$$

and

$$v'/v = \sqrt{V'/V} \ . \tag{3b}$$

The square root of the electrical potential in charged particle optics plays the role of the index of refraction in light optics. The same relations can be obtained by application of the principle of least time in the light optics case and least action in the charged particle optics case.

B. Photometry

Consider an element of area da of a surface at potential V from which charged particles are being emitted. If all the particles leaving da arrive at da' at potential V', the linear magnification of the system, M, is $\sqrt{da'/da}$. The total current, i, from da into a cone of half angle Θ is got by integrating the current density, j, as a function of angle over Θ.

$$i = \int j \cos \Theta \, da \sin \Theta d\Theta d\phi \tag{4a}$$

$$i = \pi j \sin^2 \Theta \, da \ . \tag{4b}$$

At da'

$$i' = \pi j' \sin^2 \Theta' \, da' \tag{4c}$$

$$i' = \pi j' \sin^2 \Theta' \, M^2 \, da \tag{4d}$$

In terms of the charge density, j_o , these relations become

$$j = j_o f(v) v dv \tag{5a}$$

and

$$j' = j_o f(v') v' dv' \tag{5b}$$

where v and v' are the particle velocities at da and da' and $f(v)$ and $f(v')$ are the corresponding distribution functions. Since the current from da all passes into da'

$$j \sin^2 \Theta = M^2 j' \sin^2 \Theta' \tag{6a}$$

$$\sin^2 \Theta \, f(v) dv = M^2 \sin^2 \Theta' f(v') dv' \tag{6b}$$

The distribution functions $f(v)$ and $f(v')$ are the Maxwellian distributions and depend only on the temperature and the potential in which the particle finds itself, therefore

$$f(v)dv/f(v')dv' = V/V' \tag{7a}$$

$$V \sin^2 \Theta = M^2 \sin^2 \Theta' \, V' \tag{7b}$$

$$V^{1/2} \sin \Theta = M \, V'^{1/2} \sin \Theta' \, . \tag{7c}$$

For Θ and Θ' small, $\sin \Theta \sim \Theta$, $\Theta' \sim \Theta'$ and

$$\Theta = M\Theta'(V'/V)^{1/2}. \tag{8}$$

As an example of the application of this formula it was desired to decelerate an ion beam in such a manner as to preserve the angular spread from the object at the image, i.e. $\Theta = \Theta'$ and $V' < V$. The above relation shown that it can be done but at the expense of the size of the image.

C. Phase Space

General treatments of particle dynamics usually begin with the construction of a Hamiltonian for the system. For a particle moving in a three dimensional cartesian coordinate system, the motion of a particle is completely specified if we know the values of the coordinates and conjugate momenta. This information can be represented by a single point in six dimensional phase space. A particle beam is therefore represented by a collection of points in phase space. For a beam of finite dimensions the phase space points will lie within a six dimensional hypervolume in phase space.

Under the action of forces which can be derived from a Hamiltonian the motion of a group of particles is such that the local density of the representative points in phase space remains constant. This is a statement of Liouville's theorem and for most purposes is valid since such a Hamiltonian can be constructed and is equal to the total energy function for static conservative field when there are no interactions between the particles. Certain simplifications occur when considering charged particle beams:

1. Generally motion in the x,y, and z directions is independent and the phase space motion can be confined to the (x,p_x), (y,p_y) and (z,p_z) planes with the areas occupied by the representative particles in each plane remaining constant.

2. If, p_z , the axial momentum is constant, then the ratio of the axial momentum to the transverse momentum, p_x/p_z , is equal to the angle the trajectory of the particle makes to the z-axis, x' . The coordinates of the 2 dimensional phase space can then be taken to be x and x'. As an example consider the two dimensional phase space defined by two slits of height $2m$ and $2n$ separated by a distance t . The figures below represent the extreme trajectories A,B,C,D of a beam in coordinate space and the representation in x,x' phase space of the beam at the two slits.

The corners of the phase space diagrams give the positions and trajectory angles of the extreme rays A,B,C,D. If there is no loss of particles between the slits the areas of the phase space diagrams will be constant as a direct consequence of Louville's theorem. When considering beam transport devices the terms acceptance and emittance are often used. Acceptance refers to an optical element and is the area of phase space containing all particles transmitted by the element. Emittance is the phase space area of the beam. For an optical element to transmit 100% of a particle beam the acceptance of the element must be greater than the emittance of the beam as well as having the correct shape.

D. Matrices

The behavior of many beam transport elements can be obtained by considering only the first order terms in the dynamics. This means that the displacement, x_2, and angular divergence, x'_2, of a particle leaving an optical element can be expressed in terms of the corresponding quantities, x_1 and x'_1, at the input to the device. In terms of matrices we can write

$$\begin{bmatrix} x_2 \\ x'_2 \end{bmatrix} = \begin{bmatrix} a_{11} & a_{12} \\ a_{21} & a_{22} \end{bmatrix} \begin{bmatrix} x_1 \\ x'_1 \end{bmatrix}. \qquad (9)$$

If more than one optical element is involved we will have a matrix for each element. From Liouville's theorem, areas in phase space remain constant. As a consequence det [ ] = 1 . This is good check on the correctness of any matrix used to represent an optical element.

III. Examples Specific Devices

A. Lenses and Imaging

The approximation that only first order terms in displacement, x, and angles, x', are sufficient to characterize optical elements is called the Gaussian approximation. To characterize the first order properties of Gaussian systems it is necessary to determine the values of the matrix elements. Consider some common situations:

1. Drift length, t.

$$x_1' = x_2'$$
$$x_2 = x_1 + tx_1'$$

The matrix representation is

$$\begin{bmatrix} x_2 \\ x_2' \end{bmatrix} = \begin{bmatrix} 1 & t \\ 0 & 1 \end{bmatrix} \begin{bmatrix} x_1 \\ x_1' \end{bmatrix}. \tag{10}$$

2. Thin lens - refraction at equipotential surfaces. In this case the change in the angle of the trajectory of the particle is proportional to the displacement of the trajectory from the axis.

$$x_2 = x_1$$
$$x_2' = x_1' - \alpha x_1$$
$$x' = -\alpha x_1$$

where α is related to the focal length of the lens. For a single refraction the matrix equation is

$$\begin{bmatrix} x_2 \\ x_2' \end{bmatrix} = \begin{bmatrix} 1 & 0 \\ -\alpha & 1 \end{bmatrix} \begin{bmatrix} x_1 \\ x_1' \end{bmatrix}. \tag{11}$$

For a lens of negligible thickness there will be refraction of two surfaces and the matrix equation is

$$\begin{bmatrix} x_2 \\ x_2' \end{bmatrix} = \begin{bmatrix} 1 & 0 \\ -(\alpha_1+\alpha_2) & 1 \end{bmatrix} \begin{bmatrix} x_1 \\ x_1' \end{bmatrix} \tag{12}$$

where $\alpha_1 + \alpha_2$ are related to the focal length of the lens.

3. Thick lens. For most electron optical lenses the focal lengths are comparable to the physical dimensions of the lens and the thin lens matrix equation is not applicable. For the thick lens, refraction at the first surface is followed by a drift length, t , and refraction at the second surface.

$$\begin{bmatrix} x_2 \\ x_2' \end{bmatrix} \quad \begin{bmatrix} 1 & 0 \\ -\alpha_2 & 1 \end{bmatrix} \begin{bmatrix} 1 & t \\ 0 & 1 \end{bmatrix} \begin{bmatrix} 1 & 0 \\ -\alpha_1 & 1 \end{bmatrix} \begin{bmatrix} x_1 \\ x_1' \end{bmatrix} \tag{13}$$

$$\begin{bmatrix} x_2 \\ x_2' \end{bmatrix} = \begin{bmatrix} 1-\alpha_1 t & t \\ \alpha_1\alpha_2 t-(\alpha_1+\alpha_2) & 1-\alpha_2 t \end{bmatrix} \begin{bmatrix} x_1 \\ x_1' \end{bmatrix} \tag{14}$$

4. Object and image spaces. Consider an object at a distance ℓ_1 , from the first refracting surface of a thick lens of thickness, t . Let the image be at a distance ℓ_2 from the second refracting surface. By convention ℓ_1 is negative since it is measured from right to left. Decomposing the system into its components we have the following matrix equations:

From the object to the first refracting surface:

$$\begin{bmatrix} x_2 \\ x_2' \end{bmatrix} = \begin{bmatrix} 1 & -\ell_1 \\ 0 & 1 \end{bmatrix} \begin{bmatrix} x_1 \\ x_1' \end{bmatrix} \tag{15a}$$

The thick lens:

$$\begin{bmatrix} x_3 \\ x_3' \end{bmatrix} = \begin{bmatrix} 1-\alpha_1 t & t \\ -(\alpha_1+\alpha_2)+\alpha_1\alpha_2 t & 1-\alpha_2 t \end{bmatrix} \begin{bmatrix} x_2 \\ x_2' \end{bmatrix} \tag{15b}$$

From the second refracting surface to the object:

$$\begin{bmatrix} x_4 \\ x_4' \end{bmatrix} = \begin{bmatrix} 1 & \ell_2 \\ 0 & 1 \end{bmatrix} \begin{bmatrix} x_3 \\ x_3' \end{bmatrix} \tag{15c}$$

The composite system is therefore

$$\begin{bmatrix} x_4 \\ x_4' \end{bmatrix} = \begin{bmatrix} 1 & \ell_2 \\ 0 & 1 \end{bmatrix} \begin{bmatrix} 1-\alpha_1 t & t \\ \alpha_1\alpha_2 t-\alpha_1-\alpha_2 & 1-\alpha_2 t \end{bmatrix} \begin{bmatrix} 1 & -\ell_1 \\ 0 & 1 \end{bmatrix} \begin{bmatrix} x_1 \\ x_1' \end{bmatrix} \tag{15d}$$

The elements in the thick lens matrix are often called the Gaussian constants, they are $-a, b, c, -d$. The negative signs are of historical origin,

$$-a = \alpha_1\alpha_2 t - \alpha_1 - \alpha_2 \tag{16a}$$

$$b = 1-\alpha_2 t \tag{16b}$$

$$c = 1-\alpha_1 t \tag{16c}$$

$$-d = t \tag{16d}$$

In terms of the Gaussian constants the composite system can be written

$$\begin{bmatrix} x_4 \\ x_4' \end{bmatrix} = \begin{bmatrix} c-a\ell_2 & -c\ell_1+b\ell_2+a\ell_1\ell_2-d \\ -a & b+a\ell_1 \end{bmatrix} \begin{bmatrix} x_1 \\ x'_1 \end{bmatrix} \tag{17}$$

Interpretation of matrix elements.

1. Imaging occurs when the size of the image is independent of the angle of the ray from the object, when, i.e. $x_4 = a_{11}x_1$ and $a_{12} = 0$.

Then $$-c\ell_1 + b\ell_2 + a\ell_1\ell_2 - d = 0 \tag{18a}$$

and $$\ell_1 = \frac{(d-b\ell_2)}{(a\ell_2-c)} \quad , \quad \ell_2 = \frac{d+c\ell_1}{a\ell_1+b} \tag{18b}$$

The linear magnification, M , is the ratio of image to object size.

$$M = x_4/x_1 = (c-a\ell_2) \tag{19}$$

Since det [ ] = 1 , $a_{22} = -1/M$ and the composite matrix is

$$\begin{bmatrix} M & 0 \\ -a & 1/M \end{bmatrix} \tag{20}$$

2. Those planes which are images of each other with unit magnification are the principal planes. Under these conditions

$$M = c-a\ell_{2H} = 1 \quad , \quad \ell_{2H} = (c-1)/a \tag{21a}$$

$$1/M = b+a\ell_{1H} = 1 \quad , \quad \ell_H = (1-b)/a \tag{21b}$$

where ℓ_{1H} and ℓ_{2H} ate the positions of the principal planes.

3. If we measure object and image distances from the principal planes rather than refracting surfaces

$$\ell_1 = \ell_{1H} + s_1 \text{ and } \ell_2 = \ell_{2H} + s_2 \tag{22}$$

where s_1 and s_2 are the distances from the object and image to the respective principal planes.

Substituting for ℓ_{1H} and ℓ_{2H}

$$M = c - a(\ell_{2H}+s_2) \qquad \frac{1}{M} = b + a(\ell_{1H}+s_1)$$

$$= c - a(\frac{c-1}{a} + s_2) \qquad = b + a(1-b/a+s_1)$$

$$= c - c + 1 - as_2 \qquad = b + 1-b + as_1$$

$$M = 1 - as_2 \qquad \frac{1}{M} = 1 + as_1 \qquad (23a,b)$$

and the composite matrix is

$$\begin{bmatrix} 1-as_2 & 0 \\ -a & 1+as_1 \end{bmatrix} . \qquad (24)$$

Since det [ ] = 1 ,

$$(1-as_2)(1+as_1) = 1$$

$$1 + as_1 - as_2 - a^2 s_i s_2 = 1 \qquad (25)$$

$$\frac{1}{s_2} = \frac{1}{s_1} + a$$

which is the commonly known lens formula.

4. Interpretation of paraxial Gaussian constants.

Consider the situation where the object is at infinity, then

$$s_1 = \infty , \quad a = 1/s_2 .$$

The value of s_2 for $s_1 = \infty$ is called the front focal length and is denoted by f_2 . Similarly for $s_2 = \infty$, $s_1 = f_1$, the rear focal length. Since the refracting surfaces for ion-optical lenses are not sharp they cannot be taken as reference points. The geometrical midpoint is used as a reference point. In measuring distances from the mid reference plane the composite matrix becomes

$$\begin{bmatrix} (X_2' - F_2)/-f_2 & (X_1' - F_2)/-f_2 + f_1 \\ -1/f_2 & (X_1' - F_1)/-f \end{bmatrix} \tag{27}$$

where

X_1', X_2' object and image distances from reference plane

F_1, F_2 focal distances from reference plane

There are published curves for f_1, f_2, F_1 and F_2 as a function of lens geometry and voltage ratios. These curves are to be used in the design of charged particle electrostatic lenses. For combinations of lenses the appropriate matrices must be multiplied together.

B. Dispersive elements. A common dispersive element in ion optics at low energies is the electrostatic energy analyzer. Most analyzers bend the charged particles through a predetermined angle and the position of the particle at the exit plane is a function of its energy. It is necessary to consider not only the plane in which the deflection is taking place, but the plane perpendicular to it. The usual first order treatment begins with the calculation of the trajectory of the central orbit through the analyzer. Then the trajectory of a particle with slightly different energy is calculated. Since the two particles will traverse different parts of the field it is usual to express the field away from the central orbit in a series expansion about the field at the central orbit and drop terms higher than the first. Two common type of electrostatic analyzers are the cylindrical and spherical analyzer. For an analyzer in which the

central orbit has a radius r_o for a particle of energy E_o the equation for the displacement, r_2, and angle, r_2', of the trajectory of an arbitrary particle of the same energy with respect to the central trajectory is

$$\begin{bmatrix} r_2 \\ r_2' \end{bmatrix} = \begin{bmatrix} \cos Q_r\alpha & r_o Q_r^{-1}\sin Q_r\alpha \\ -Q_r r_o^{-1}\sin Q_r\alpha & \cos Q_r\alpha \end{bmatrix} \begin{bmatrix} r_1 \\ r_1' \end{bmatrix} \qquad (28)$$

where r_1 and r_1' are the initial displacement and angle and $Q_r^2 = 3-N$ for $N = -(r_o/E_o)\partial E/\partial r$. For the field between two cylinders $N = 1$ for two spheres $N = 2$. The total angle through which the particles are deflected is α. From the definition of focus, we see that first order focusing will occur when $\sin Q_r\alpha = 0$. For a cylindrical analyzer this will be the case when $\alpha = \pi/\sqrt{2}$. For the spherical analyzer the focussing condition is met when $\alpha = \pi$. The matrix representation of the trajectory of a particle with kinetic energy $E_o + \Delta E$ is

$$\begin{bmatrix} r_2 \\ r_2' \\ \frac{\Delta E}{E_o} \end{bmatrix} = \begin{bmatrix} \cos Q_r\alpha & Q_r^{-1} r_o \sin Q_r\alpha & Q_r^{-2} r_o[1-\cos Q_r\alpha] \\ -Q_r r_o^{-1}\sin Q_r\alpha & \cos Q_r\alpha & Q_r^{-1}\sin Q_r\alpha \\ 0 & 0 & 1 \end{bmatrix} \begin{bmatrix} r_1 \\ r_1' \\ \frac{\Delta E}{E_o} \end{bmatrix} \qquad (29)$$

The values of the matrix elements in the bottom row reflect the fact that the analyzer does not change the energy of the particles. The element a_{13} gives the displacement as a function of ΔE and is commonly called the dispersion of the analyzer.

IV. Charged Particle Trajectories in Crossed Electric and Magnetic Fields.

The motion of charged particles traveling with non-relativistic energies in crossed electric and magnetic fields has been investigated by Hanneberg[1] and by Millett[2] for particles with relativistic energies. Derivations for the special configuration of the superposition of the electric field E of a parallel plate condenser and a homogeneous magnetic field B directed along the vertical dimension of the plates have been published by several authors[3,4,5] and applied to the design of velocity filters. The purpose of this derivation is to obtain general analytic first order expressions in a convenient matrix form for the motion of charged particles with non-relativistic energies in crossed electric and magnetic fields. The derivation follows closely the derivations for the motion of charged particles in electric and magnetic fields given by Banford.[6] Using the matrix formulation, design parameters for a velocity filter will be calculated.

---

1. W. Hanneberg, Ann. Physik 19, 335 (1934).
2. W.E. Millett, Phys. Rev. 74, 1058 (1948).
3. W. Wien, Ann. Physik 65, 444 (1898); 8, 260 (1902).
4. E.B. Jordan, Phys. Rev. 58, 1009 (1940); 60, 710 (1941).
5. K.W. Ogilvie, R.I. Kittredge and T.D. Wilkerson, Rev. Sci Instr. 39, 453 (1968).
6. A.P. Banford, The Transport of Charged Particle Beams, E. and F.N. Spon, Ltd., London, 1966, Chapter 5.

The field configuration considered is the superposition of the electric field E of a cylindrical condenser and a homogeneous magnetic field B directed parallel to the cylinder axis. The equations of motion will be described in terms of cylindrical coordinates with the origin at the center of curvature of the condenser. Initially, we shall only be concerned with trajectories perpendicular to the plane of the condenser plates. In such a field a particle of mass $\underline{m}$, charge Ze, and velocity v_o will travel along a circular orbit of radius r_o where the centrifugal force on the particle is balanced by the electric and magnetic forces

$$mv_o^2/r_o = ZeE_o + ZeB_o v_o \tag{1}$$

$$ZeE_o/mv_o^2 = 1/r_o - ZeB_o/mv_o \tag{2}$$

where E_o and B_o are the values of the electric and magnetic fields at r_o.

At radius $r_o + \underline{r}$ the electric field is E_r and to first order the potential is rE_o. The kinetic energy of the particle at this point is less than the kinetic energy at radius r_o by an amount $ZerE_o$. Thus

$$mv_r^2/2 = mv_o^2/2 - ZerE_o \tag{3}$$

$$v_r^2 = v_o^2(1 - 2ZeE_o r/mv_o^2) \tag{4}$$

and substituting from equation (2) for ZeE_o/mv_o^2 we have

$$v_r^2 = v_o^2(1 - 2r/r_o + 2ZeB_o r/mv_o) \ . \qquad (5)$$

The radial equation of motion is

$$m\ddot{r} = mv_r^2/(r_o+r) - ZeE_r - Zev_r B_r \ . \qquad (6)$$

E_r and B_r, the fields at $r_o + r$ can be expressed in terms of E_o and B_o and their radial derivatives giving the relations

$$E_r = E_o + r\partial E/\partial r \qquad (7a)$$

$$B_r = B_o + r\partial B/\partial r \qquad (7b)$$

where the partial derivatives are evaluated at r_o. By introducing the electric field index $N = -(r_o/E_o)\partial E/\partial r$ and the magnetic field index $n = -(r_o/B_o)\partial B/\partial r$, (7a) and (7b) can be rewritten as

$$E_r = E_o(1 - Nr/r_o) \qquad (8a)$$

$$B_r = B_o(1 - nr/r_o) \ . \qquad (8b)$$

Putting these expressions into (6) we have

$$m\ddot{r} = mv_r^2/r_o^2(r_o-r) - ZeE_o(1-Nr/r_o) - Zev_r B_o(1-nr/r_o) \ . \qquad (9)$$

Substituting the expression for v_r and expanding

$$m\ddot{r} = mv_o^2/r_o^2(1-2r/r_o + 2ZeB_or/mv_o)(r_o-r) - ZeE_o(1-Nr/r_o) - ZeB_ov_o(1-2r/r_o + 2ZeB_or/mv_o)^{1/2}(1-nr/r_o) . \quad (10)$$

Expanding the square root term and cancelling

$$\ddot{r} = (N-3)v_o^2r/r_o^2 + (n-N+3)ZeB_ov_or/mr_o - Z^2e^2B_o^2r/m^2 - (n+2)ZeB_ov_or^2/mr_o^2 + 2v_o^2r^2/r_o^3 + nZ^2e^2B_o^2r^2/m^2r_o^2 . \quad (11a)$$

Considering only those terms first order in r

$$\ddot{r} = [(N-3)v_o^2/r_o^2 + (n-N+3)ZeB_ov_o/mr_o - B_o^2e^2/m_2]r . \quad (11b)$$

It is now convenient to change the independent variable from time to distance along the orbit, z .

$$\dot{r} = (dr/dz)\dot{z} \quad , \quad \ddot{r} = (dr/dz)\ddot{z} + (d^2r/dz^2)\dot{z}^2 .$$

Denoting d/dz by a prime and setting $\dot{z}$ equal to v_o equation (11b) can be rewritten

$$\ddot{r} = [(N-3)/r_o^2 + (n-N+3)ZeB_o/mv_or_o - B_o^2e^2/m^2v_o^2]r \quad (12)$$

which has the solution

$$r = A \cos Qz + B \sin Qz \tag{13}$$

where $Q = [(3-N)/r_o^2 + (N-n-3)ZeB_o/mv_o r_o + Z^2e^2B_o^2/m^2v_o^2]^{1/2}$ and A and B are constants of integration to be determined from the initial conditions. The displacement of the orbit from the central orbit is $\underline{r}$ while r' is the angle the orbit makes with the central orbit. If we set $\underline{r} = r_1$ and $r' = r_1'$ when $z = 0$, then $A = r_1$. Letting r_2 and r_2' be the values of $\underline{r}$ and r' at $\underline{z}$ gives $B = r_1'/Q$. The equations for r_2 and r_2' are

$$r_2 = r_1 \cos Qz + (r_1'/Q)\sin Qz \tag{14a}$$

$$r_2' = -r_1 Q \sin Qz + r_1' \cos Qz \ . \tag{14b}$$

In matrix form the equations become

$$\begin{bmatrix} r_2 \\ r_2' \end{bmatrix} = \begin{bmatrix} \cos Qz & (1/Q)\sin Qz \\ -Q \sin Qz & \cos Qz \end{bmatrix} \begin{bmatrix} r_1 \\ r_1' \end{bmatrix} \tag{15}$$

Equations 14a, 14b, and 15 all apply to particles with the same momentum and energy. If we allow for particles with momenta and energies different from those of the central particle, the equations will have to be modified.

If the momentum of the particle with equilibrium orbit of radius r_o is $\underline{p}$, then the equilibrium orbit for a particle of momentum $\underline{p} + \Delta p$ will have a radius $r_o + \Delta r_o$. Rewriting (2) in terms of $\underline{p}$ we have

$$r_o = p^2/(mE_o + pB_o)Ze \tag{16}$$

and at $r_o + \Delta r_o$

$$r_o + \Delta r_o = (p+\Delta p)^2/[mE_r + (p+\Delta p)B_r]Ze \tag{17}$$

Using the expressions for E_r and B_r given in 8a and 8b

$$r_o + \Delta r_o = p^2(1+\Delta p/p)^2/[mE_o(1-N\Delta r_o/r_o) + pB_o(1+\Delta p/p)(1-n\Delta r_o/r_o)]Ze \tag{18}$$

Dividing (18) by (16) and keeping only first order terms

$$1 + r/r_o = \frac{1 + 2\Delta p/p}{\dfrac{mE_o(1-N\Delta r_o/r_o) + pB_o(1+\Delta p/p-n\Delta r_o/r_o)}{(mE_o + pB_o)}} \tag{19}$$

Dividing out the denominator and expanding

$$1 + \Delta r_o/r_o = \frac{1 + 2\Delta p/p}{1 - N\Delta r_o/r_o + pB_o[\Delta p/p + (N-n)\Delta r_o/r_o]/(mE_o+pB_o)} \tag{20}$$

$$1 + \Delta r_o/r_o = (1+2\Delta p/p)\{1-N\Delta r_o/r_o + pB_o[\Delta p/p + (N-n)\Delta r_o/r_o]/(mE_o+pB_o)\}$$

$$1 + \Delta r_o/r_o = 1 - N\Delta r_o/r_o + [\Delta p/p+(N-n)\Delta r_o/r_o]pB_o/(mE_o+pB_o) + 2\Delta p/p$$

or

$$\Delta r_o/r_o = 2\Delta p/p - N\Delta r_o/r_o + pB_o[\Delta p/p + (N-n)\Delta r_o/r_o]/(mE_o+pB_o) \tag{21}$$

For the case of uniform electric and magnetic fields $N = n = 0$ and

$$\Delta r_o/r_o = \Delta p/p[2 + pB_o/(mE_o+pB_o)] \tag{22}$$

The first term of the RHS of (22) is that given by Millett[2] for the velocity dispersion. Considering only this first term the values of r_2 and r_2' can now be written in terms of r_1 , r_1' , r_o and $\Delta p/p$. If $\underline{r}$ is the displacement of a particle from the central ray (for which $\Delta p = 0$) , its displacement from its own equilibrium orbit will be $r - \Delta r_o$. Under these conditions

$$r_2 - 2r_o\Delta p/p = (r_1-2r_o\Delta p/p) \cos Qz + r_1'(1/Q) \sin Qz \tag{23a}$$

$$r_2' = (r_1-2r_o\Delta p/p)(-Q \sin Qz) + r_1' \cos Qz \tag{23b}$$

In matrix form this becomes

$$\begin{bmatrix} r_2 \\ r_2' \\ \Delta p/p \end{bmatrix} = \begin{bmatrix} \cos Qz & (1/Q) \sin Qz & 2r_o(1-\cos Qz) \\ -Q \sin Qz & \cos Qz & 2r_o\, Q \sin Qz \\ 0 & 0 & 1 \end{bmatrix} \begin{bmatrix} r_1 \\ r_1' \\ \Delta p/p \end{bmatrix} \tag{24}$$

To apply these formulae to the parallel plate velocity filter we take the limit of Q as $r_o \to \infty$ for $N = 0$ and let $\underline{z}$, the distance along the orbit, be equal to L the length of the filter.

$$Q = ZeE_o/mv_o^2 = ZeE_o/2T \tag{25}$$

Letting $B_o = E_o/v_o$

$$1/r_o = ZeE_o/2T + ZeB_o/2T$$
$$r_o = T/ZeE_o \ . \tag{26}$$

If y is now the displacement from the straight-through orbit in the filter and y' the angle of the orbit with respect to the filter axis

$$\begin{bmatrix} y_2 \\ y_2' \\ \Delta p/p \end{bmatrix} = \begin{bmatrix} \cos L/2r_o & 2r_o \sin L/2r_o & 2r_o(1-\cos L/2r_o) \\ -1/2r_o \sin L/2r_o & \cos L/2r_o & \sin L/2r_o \\ 0 & 0 & 1 \end{bmatrix} \begin{bmatrix} y_1 \\ y_1' \\ \Delta p/p \end{bmatrix}. \tag{27}$$

The momentum dispersion is given by $2r_o(1-\cos L/2r_o)$ and is a maximum for $\cos L/2r_o = -1$ or $L/2r_o = \pi$. Let the length which gives maximum dispersion be L_o , then $L_o/2r_o = \pi$ and $1/2r_o = \pi/L_o$. Equation (27) can now be rewritten in terms of L_o

$$\begin{bmatrix} y_2 \\ y_2' \\ \Delta p/p \end{bmatrix} = \begin{bmatrix} \cos \pi L/L_o & (L_o/\pi) \sin \pi L/L_o & (L_o/\pi)(1-\cos \pi L/L_o) \\ -\pi/L_o \sin \pi L/L_o & \cos \pi L/L_o & \sin \pi L/L_o \\ 0 & 0 & 1 \end{bmatrix} \begin{bmatrix} y_1 \\ y_1' \\ \Delta p/p \end{bmatrix}.$$

The length L_o which gives the maximum dispersion all corresponds to the length where first order focussing occurs, i.e. where y_2 is independent of y_1' .

V. Design Parameters for the Wien Filter

To calculate the performance of an actual Wien filter it is first necessary to establish the range of physical conditions under which it is to operate. For the study of the ion composition of the solar wind the range to be covered is 1.0 to 4.5 (see Table I) while the velocities of the ions are in the range 300-600 km/sec. The length, L, of the filter will be fixed as will be the magnetic field, B_o, while, L_o, the length at which first order focussing occurs depends on M/Z and v_o, the velocity of the ion.

$$L_o = \frac{\pi u}{e} \frac{M}{Z} \frac{v_o}{B_o} \text{ m}$$

$$L_{o_{min}} = \frac{u}{e} \cdot \frac{\pi}{B_o} \cdot 3\text{x}10^5 \text{ m}$$

$$L_{o_{max}} = \frac{4.5u}{e} \frac{\pi}{B_o} \text{ x } 6\text{x}10^5 \text{ m}$$

where u is the atomic mass unit. The ratio $L_{o_{min}}/L_{o_{max}} = .111$ To insure that no ion will make more than a single complete oscillation when traversing the filter L is chosen equal to $L_{o_{min}}$. As a result, the ratio L/L_o will vary from a maximum of 1 (for $M/Z = 1$ and $v_o = 3\text{x}10^5$ m/sec). It is now possible to calculate the displacement of an ion from the axis of the filter as a function of L/L_o, y_1, the entrance angle, and $\Delta p/p$, the fractional deviation of the ion momentum from the momentum corresponding to first order focussing at $L/L_o = 1$. Under the conditions which prevail in the solar wind

at any instant where all ions have the same velocity and $\Delta p/p$ is equivalent to $\Delta M/M$, the mass resolution. Plots of y_2/L_o, the reduced ion displacement, as a function of L/L_o for entrance angles from 0° to 5° are shown in Figures 1-6 for $\Delta M/M = 0.00$, 0.01, 0.02, 0.03, 0.04, and 0.05. The curves correspond to ion trajectories passing through the center of the entrance aperatur, i.e., $y_1/L = 0$. From these plots, it is possible to establish a measure of the resolution of the filter over any given range of L/L_o and entrance angle, y_1', by determining the value of L/L_o for which the $y_1' = 0$ curve for a given set of $\Delta M/M$ curves crosses the curves for $\Delta M/M = 0$ at different entrance angles. This is most easily done by superposing the $\Delta M/M = 0$ curves over the curves for the other values of $\Delta M/M$. The results are tabulated in Table II along with the maximum value of the off-axis coefficient, $\cos \pi L/L_o$, corresponding to the minimum value of L/L_o, the minimum value of the coefficient is -1 corresponding to $L/L_o = 1$.

From the values in Table II it is clear that the required L/L_o range will not be able to be covered at the angles and resolutions considered. Figure 6 is a plot of the reduced displacement of the ion trajectories as a function of L/L_o for angles of incidence of 1° and less where $\Delta M/M = 0$. Superimposed on this plot are the $y_1' = 0$ curves for $\Delta M/M$ values from .01 to .05. The intersection points of the curves represent the values of L/L_o for which trajectories for ions with the different $\Delta M/M$ values are displaced by the same distance as the $\Delta M/M = 0$ trajectories as

a function y_1' trajectory for the $\Delta M/M = 0$ trajectory. The L/L_o values at the intersection points are listed in Table III for trajectories where $y_1/L_o = 0$. If we relax the restriction on the M/Z range from 1-4.5 to 1.5-4.5 and consider only solar wind velocities below 5×10^5 m/sec. the values of L/L_o falling below the solid define the appropriate combination of mass and angular resolution.

To select the optimum combination of mass and angular resolution it is necessary to consult Table IV where the expected species and charge states of the solar wind ions are arranged in order of increasing M/Z. The third and fourth columns respectively show the abundance of the species and the resolution $\Delta(M/Z)/(M/Z)$ required to separate each from the next in order. A resolution of approximately .01 is required to fully resolve all the species, however with a resolution of .03 it would be possible to resolve He, C, O, Ne, Si and Fe and obtain charge distributions for C, O, and Fe. With a resolution of .03 an incoming particle angle of $\pm .6^\circ$ can be accommodated and a five-fold range in L/L_o covered (see Table III).

The dimensions of the filter can be fixed by considering the sensitivity required. Assuming the filter to be located on a spinning spacecraft, with a period of revolution of 3 seconds, the flux of protons entering the filter per revolution is

$$F = \frac{2 \times 10^8 \times 3 \times A \times \delta}{2\pi}$$

where δ is the angular width of the solar wind velocity distribution, which we assume to be of order 0.1, and A is the area of the entrance aperture. If we require a species having an abundance relative to H^+

of 3×10^{-6} to yield 4 particles per revolution then A = .15 cm^2.

Consider a filter of length L = 15 cm. the maximum exit slit half width for such a filter fulfilling the resolution requirements discussed above for L/L_o = .2 is $(y_2/L_o) \times L_o$ where y_2/L_o = .002 and L_o = 75 cm. giving y_2 = .15 cm. and a full width of .30 cm. This analysis applies to an entrance slit of negligible width since off axis trajectories have not been considered. When these trajectories are taken into account it is necessary to restrict the width of the exit slit for finite entrance slit width. A reasonable compromise has exit and entrance slits of equal widths to 0.15 cm. The condition for an entrance slit area of .15 cm^2 can then be met with an entrance slit height of 1.0 cm.

The angular acceptance in the vertical plane is determined by geometrical considerations alone for the conventional Wien filter. If particles passing through the center of the entrance slit with a maximum angle of 5° are to be accepted by the exit slit, the exit slit full height must be $2 \times 15 \tan 5° = 2.6$ cm.

The final design parameters to be determined are the magnetic and electric fields. The magnetic field is chosen so that the particle with the smallest M/Z value traveling at its minimum velocity will oscillate no more than one half cycle in passing through the filter. Setting L_o = 15 cm corresponding to L/L_o = 1

$$B_o = \left(\frac{M}{Z}\right)_{min} \frac{V_{min}}{15} \frac{\pi u}{e}$$

$$= 978 \text{ gauss} .$$

The maximum electric field occurs for ions with the maximum velocity

and is given by

$$E_{max} = B_o v_{max}$$

$$= 489 \text{ volts/cm} .$$

A summary of the Wien filter parameters as discussed above is presented in the first column of Table IV.

An improvement in the performance of the plane parallel plate Wien filter can be made if the electric field plates are curved as suggested by Legler.[7] The curved plate design permits focussing in both the vertical and horizontal planes of the filter, hence the name stigmatic Wien filter. To be consistent with the previous results only the first order theory is used. A disadvantage of the stigmatic filter is its focussing length which is longer than the ordinary filter by a factor of $\sqrt{2}$; the dispersion for the two filters is identical. The transfer matrix for motion in the vertical plane of the stigmatic filter is

$$\begin{bmatrix} x_2 \\ x_2' \end{bmatrix} \qquad \begin{bmatrix} \cos \pi L/L_o & (L_o/\pi) \sin \pi L/L_o \\ -\pi/L_o \sin \pi L/L_o & \cos \pi L/L_o \end{bmatrix} \begin{bmatrix} x_1 \\ x_1' \end{bmatrix}$$

where here L_o is $\sqrt{2}$ times the value for the ordinary filter. The maximum excursion of the particle trajectory in the vertical plane passing through the center of entrance slit at an angle of 5° from horizontal occurs when $L_o = L/2$ and is equal to $(L/2)(5/180) = .294$ cm.

---

[7] W. Legler, Z. Phys., 171, 424 (1963).

The maximum full exit slit height is therefore .59 cm. An exit slit height of 1.0 cm could accommodate particles passing through the center of the entrance slit with angles to the horizontal of as much as 8.5°. With the stigmatic filter one therefore gains vertical angular acceptance and a reduction in the vertical height of the analyzer at the price of increased filter length. The design parameters for the stigmatic filter are listed in the second column of Table IV.

VI. Electrostatic Energy Analyzer Design.

An unambiguous measurement of M/Z for an ion requires not only the determination of the velocity of the ion per unit charge but also its energy per unit charge. For this reason the Wien filter described above must be preceded by an energy analyzer. The most suitable energy analyzer for this application is the hemispherical electrostatic analyzer. It has the advantages of small size and relatively high dispersion and uses voltages which are low compared to the voltages of the ions to be analyzed. Furthermore, ions incident on the entrance slit of the analyzer are focused with unit magnification on the exit slit. The transfer matrix for the hemispherical analyzer is given in equation (29) for $Q_r = 1$. The mean radius of the analyzer can be calculated once r_1 and $\Delta E/E_o$ have been determined. The equation for the displacement of the trajectory, r_2 , from the central trajectory at the exit slit of the analyzer is

$$r_2 = r_1 + (\Delta E/E_o)2r_o \ .$$

If r_2 is chosen equal to the half width of the Wien filter and $\Delta E/E_o$ equal to its resolution, for $r_1 = 0$

$$r_o = \frac{.075}{2x.03} = 1.25 \text{ cm}$$

The maximum deviation from the central trajectory occurs when

$$r_1' r_o \sin \alpha + (\Delta E/E_o)\, r_o\, (1-\cos \alpha)$$

is a maximum, or

$$r_1' \cos \alpha + (\Delta E/E_o)(\sin \alpha) = 0$$

$$\tan \alpha = - r_1'/(\Delta E/E_o)$$

and $$\alpha = 87.1^\circ .$$

The maximum deviation $r_{2_{max}}$ is given by

$$r_{2_{max}} = r_1' r_o \sin 87.1^\circ + (\Delta E/E_o) r_o (1-\cos 87.1^\circ)$$

$$= .049 \text{ cm} .$$

Taking into account the .075 cm width of the entrance slit, the maximum possible deviation of the trajectory is .124 cm, given a plate spacing of .247 cm. Increasing this figure by 30% to assure that overfilling of the analyzer will not occur, gives a final spacing of .32 cm.

The potential difference between the plates, V , given by the formula

$$V = V_o \left(\frac{R_2}{R_1} - \frac{R_1}{R_2}\right)$$

where V_o is the kinetic energy of the ions passed by the analyzer

and R_1 and R_2 are the radii of the inner and outer hemisphere respectively. For $R_1 = r_o - .16\text{cm}$ and $R_2 = r_o + .16$ cm

$$V = V_o \left[\frac{1.41}{1.09} - \frac{1.09}{1.41}\right]$$

$$= .520\ V_o \quad .$$

The maximum value of V_o occurs at M/Z = 4.5 at a velocity of 500 km/sec and is equal to approximately 8 kV. Under these conditions the maximum voltage across the analyzer plates would be 4.2 kV.

VII. Annotated Bibliography

Energy and Momentum Analysis

W.M. Brubaker and J. Tool, Rev. Sci. Instr. 35, 1007(1964)

Performance Studies of a Quadrupole Mass Filter

This is an investigation of the dependence of resolution and transmission efficiency upon entrance aperture size and frequency of excitation.

Energy and Momentum Analysis

A.E. Holme, W.J. Thatcher and J.H. Leck, J. Phys. E. 5, 433(1972)

An Investigation of the Factors Determining Maximum Resolution in a Quadrupole Mass Spectrometer

Energy and Momentum Analysis

C.E. Kuyatt and J.A. Simpson, Rev. Sci. Instr. 38,103(1967)

Electron Monochromator Design

This is particularly useful for the summaries of several of the restrictions on charged-particle beam systems which are given in section II. Details are given in part III of a spherical electrostatic energy analyzer.

Energy and Momentum Analysis

J.S. Risley, Rev. Sci. Instr. 43, 95(1972)

Design Parameters for the Cylindrical Mirror Energy Analyzer

A detailed account of the c.m.e. analyzer including calculations of trajectories, resolution, dispersion, aberrations, and the effect of a finitely extended source. A comparison with the second-order focusing of a parallel plate analyzer is also included.

Energy and Momentum Analysis

H.Z. Sar-El, Rev. Sci. Instr. 38, 1210(1967)

Cylindrical Capacitor as an Analyzer I. Nonrelativistic Part

A study of the cylindrical mirror energy analyzer

Energy and Momentum Analysis

K.D. Sevier, Low Energy Electron Spectrometer (Wiley-Interscience, New York, 1972)

Chapter 2, sections 2 and 3, give a rather compressed but complete account of magnetic and electrostatic analyzers. These sections are particularly valuable for their list of references which appears to be rather exhaustive. Note that this book is not an introductory work and seems to assume an unspecified amount of prior familiarity with the material.

Energy and Momentum Analysis

P. Staib, J. Phys.: E. 5, 484(1972)

An Improved Retarding Field Analyzer

A retarding field analyzer consisting of sections of spherical grids is described. The analyzer is of interest because it might find use as the monochromator portion of a charged particle gun.

Lenses and Focusing

A. Adams and F.H. Read, J. Phys. E5, 150(1972); 156(1972)

Electrostatic Cylinder Lenses

II. Three-element Einzel Lenses

III. Three-element asymmetric voltage lenses

Calculation of the properties of lenses consisting of three equidiameter coaxial cylinders

Lenses and Focusing

A.B. El-Karch and M.A. Sturans, J. Appl. Phys. 42, 1870(1971)

Analysis of the Three-Tube Symmetrical Electrostatic Unipotential Lens

A digital computer study of the einzel lens

Lenses and Focusing

H.B. Haskell, O. Heinz, and D.C. Lorents, Rev. Sci. Instr. 37, 607(1966)

Multistage Gun for Production of Low Energy Ion Beams

This article contains fairly detailed information about the performance of a thermal Li^+ emitter in conjunction with a two-stage electrostatic lens system. The extraction stage, a "standard Soa immersion lens", and the deceleration stage are both of simple construction. Examples of beam profiles and currents are given for several systems with final ion energies ranging from 2 to 100 eV. The final currents are usually about a factor of 30 smaller than the maximum space-charge limited current and this is attributed to the inefficiency of the source.

Lenses and Focusing

D.W.O. Heddle, J. Phys. E2, 1046(1969)

The Design of Three-Element Electrostatic Electron Lenses

A discussion of the focal properties of electron lens systems consisting of three equal diameter cylinders is given in terms of the properties of the analogous two-element lens system. Note that the definition of magnification is incorrect.

See Heddle and Kurepa, J. Phys. E3, 594(1970) for experimental verification.

Lenses and Focusing

D.W.O. Heddle and M.V. Kurepa, J. Phys. E3, 552(1970)

The Focal Properties of Three Element Electrostatic Electron Lenses

This aritcle contains the experimental verification of the disucssion of the three-tube lens of Heddle, J. Phys. E2, 1046(1964). The results are in good agreement if only paraxial rays are considered. The definition of the magnification is still incorrect, unfortunately. Also, no investigation is made of the angular properties of the beam or of the beam profile near the focus.

Lenses and Focusing

S. Natali, D. Dichio, E. Ura and C.E. Kuyatt, Rev. Sci. Instr. 43, 80(1972)

Accurate Calculation of Properties of the Two-Tube Electrostatic Lens: First-Order Focal Properties and P-Q Curves

The P-Q (object-image position) curves are recalculated for a system of two cylindrical lenses.

Lenses and Focusing

F.H. Read, J. Phys. E2, 165(1969); 2, 679(1969); 4, 562(1971)

Calculations of the properties of

a) double aperture electrostatic immersion lens
b) three-aperture einzel lens
c) 'zero gap' electrostatic aperture lenses

Lenses and Focusing

F.H.Read, A. Adams and J.R. Soto-Montiel, J. Phys. E4, 625(1971)

Electrostatic Cylinder Lenses I: Two Element Lenses

Solutions of Laplace's equation for equidiameter coaxial cylinders are obtained and used to calculate the properties of double cylinder electrostatic lenses.

Lenses and Focusing

J.A. Simpson and C.E. Kuyatt, Rev. Sci. Instr. 34, 265(1963)

Design of Low Voltage Electron Guns

In the two guns described a high voltage is utilized to overcome the space charge in front of the cathode. The electrons are then decelerated to their final energy. The first gun described has been utilized fairly successfully for the production of low energy Li^+ beams (see Haskell, et al., Rev. Sci. Instr. 37, 607(1966) for details). The second gun design involves a point-source (hairpin) cathode.

Lenses and Focusing

J.A. Simpson, Electron Guns in Method of Experimental Physics: Vol. 4 Atomic and Electron Physics: Part A: Atomic Sources and Detectors edited by V.W. Hughes and H.L. Schultz (Academic Press, New York, 1967) Section 1.1.5, pp. 84-95.

This section of the book contains a very convenient summary of the principles of electron (and ion) optics.

Electron Optics-General

P. Grivet, Electron Optics (Pergamon Press, Oxford, 1965)

This is a translation of an earlier French-language edition. The first part of the book is a detailed account of the standard topics in electron optics. The second part is concerned with actual instruments using the principles of electron and ion optics, such as cathode ray tubes, mass spectrometers, and particularly, the electron microscope.

Electron Optics-General

O. Klemperer and M.E. Barnett, Electron Optics, Third edition, (Cambridge, 1971)

This book in its third incarnation provides a convenient introduction to the physics of electron lenses and electron deflectors. There are chapters devoted to electron lens abberations, space charge, and design of electron guns.

Electron Optics-General

K.R. Spangenberg, Vacuum Tubes (McGraw-Hill, New York, 1948)

This is one of the standard works in the field. In the course of the discussion of the physics of electron tubes such topics are potential field mapping, electron motion, space-charge effects, and the characteristics of various electrostatic and magnetic lenses are considered. (Unfortunately it is probably still out of print and should be reissued.)

Electron Optics-General

J.R. Pierce, Theory and Design of Electron Beams (Van Nostrand, Princeton, 1954)

The standard topics:electron motion in fields, electrostatic and magnetic lenses, space charge. Unfortunately a bit obscure in places.

Electron Optics-General

A.P. Banford, The Transport of Charged Particle Beams (Spon, London, 1966)

This book concerns itself mostly with high-energy beam problems, but the matrix representation of charged-particle optical components given in Chapter 3 is of more general utility and is quite useful for lower energy situations.

TABLE I

SOLAR WIND COMPOSITION ARRANGED IN ORDER OF INCREASING M/Z*

Ion	M/Z	Abundance Relative to $^{1}H^{+}$	$\frac{\Delta(M/Z)}{M/Z}$
$^{1}H^{+}$	1.00	1.00×10^{12}	
$^{3}He^{+2}$	1.50	2.42×10^{7}	> .33
$^{4}He^{+2}$	2.00	8.08×10^{10}	> .42
$^{12}C^{+6}$	2.00	2.68×10^{8}	> .00
$^{14}N^{+7}$	2.00	3.24×10^{6}	> .00
$^{16}O^{+7}$	2.29	3.06×10^{7}	> .14
$^{14}N^{+6}$	2.33	3.91×10^{7}	> .017
$^{28}Si^{+12}$	2.33	1.82×10^{5}	> .00
$^{24}Mg^{+10}$	2.40	2.01×10^{7}	> .029
$^{12}C^{+5}$	2.40	2.18×10^{8}	> .00
$^{20}Ne^{+8}$	2.50	8.1×10^{7}	> .042
$^{28}Si^{+11}$	2.54	9.57×10^{5}	> .016
$^{24}Mg^{+9}$	2.67	7.31×10^{6}	> .051
$^{16}O^{+6}$	2.67	4.65×10^{8}	> .00
$^{14}N^{+5}$	2.80	5.04×10^{7}	> .060
$^{28}Si^{+10}$	2.80	5.03×10^{6}	> .00
$^{20}Ne^{+7}$	2.86	1.94×10^{6}	> .021
$^{32}S^{+11}$	2.91	3.84×10^{5}	> .032
$^{12}C^{+4}$	3.00	2.73×10^{7}	> .031
$^{24}Mg^{+8}$	3.00	3.49×10^{6}	> .00
$^{28}Si^{+9}$	3.11	1.55×10^{7}	> .036
$^{16}O^{+5}$	3.20	2.02×10^{9}	> .028
$^{32}S^{+10}$	3.20	2.92×10^{6}	> .00
$^{20}Ne^{+6}$	3.33	9.51×10^{4}	> .040
$^{24}Mg^{+7}$	3.43	1.03×10^{7}	> .029
$^{28}Si^{+8}$	3.50	1.1×10^{7}	> .020
$^{32}S^{+9}$	3.56	8.7×10^{6}	> .016
$^{24}Mg^{+6}$	4.00	7.08×10^{3}	> .11
$^{28}Si^{+7}$	4.00	3.02×10^{6}	> .00
$^{32}S^{+8}$	4.00	5.7×10^{6}	> .00
$^{56}Fe^{+14}$	4.00	4.9×10^{4}	> .072

Ion	M/Z	Abundance Relative to $^{1}H^{+}$	$\frac{\Delta(M/Z)}{M/Z}$
$^{56}Fe^{+13}$	4.31	6.8×10^{5}	> .057
$^{32}S^{+7}$	4.57	1.61×10^{6}	> .021
$^{28}Si^{+6}$	4.67	1.82×10^{5}	> .00
$^{56}Fe^{+12}$	4.67	3.6×10^{6}	> .082
$^{56}Fe^{+11}$	5.09	7.37×10^{6}	> .045
$^{32}S^{+6}$	5.33	1.84×10^{5}	> .048
$^{56}Fe^{+10}$	5.60	9.68×10^{6}	> .10
$^{56}Fe^{+9}$	6.22	7.18×10^{6}	> .11
$^{56}Fe^{+8}$	7.00	2.38×10^{6}	> .125
$^{56}Fe^{+7}$	8.00	3.2×10^{5}	

*Data from article by T. E. Holzer and W. I. Axford, "Solar Wind Ion Composition". Solar corona temperature equal to 1.26×10^{6} °K.

TABLE II

$\Delta M/M = .01$

y_1'	L/L_o range	y_2/L_o	cos $\pi L/L_o$
1°	0.66-1.0	0.0050	-.48
2°	0.82-1.0	0.0060	-.84
3°	0.88-1.0	0.0062	-.93
4°	0.91-1.0	0.0063	-.96
5°	0.92-1.0	0.0063	-.97

$\Delta M/M = .02$

y_1'	L/L_0 range	y_2/L_o	cos $\pi L/L_o$
1°	0.44-1.0	0.0052	.19
2°	0.66-1.0	0.0094	-.48
3°	0.76-1.0	0.0110	-.73
4°	0.81-1.0	0.0118	-.83
5°	0.85-1.0	0.0122	-.89

$\Delta M/M = .03$

y_1'	L/L_o range	y_2/L_o	cos $\pi L/L_o$
1°	0.34-1.0	0.0050	.48
2°	0.56-1.0	0.0112	-.19
3°	0.67-1.0	0.0144	-.51
4°	0.75-1.0	0.0160	-.71
5°	0.80-1.0	0.0170	-.81

$\Delta M/M = .04$

y_1'	L/L_o range	y_2/L_o	cos $\pi L/L_o$
1°	0.28-1.0	0.0045	.64
2°	0.46-1.0	0.0108	.12
3°	0.58-1.0	0.0158	-.25
4°	0.67-1.0	0.0190	-.51
5°	0.73-1.0	0.0208	-.66

$\Delta M/M = .05$

y_1'	L/L_o range	y_2/L_o	cos $\pi L/L_o$
1°	0.20-1.0	0.0033	.81
2°	0.38-1.0	0.0100	.37
3°	0.51-1.0	0.0163	-.03
4°	0.60-1.0	0.0208	-.31
5°	0.67-1.0	0.0238	-.51

TABLE III

$\Delta M/M$	y_1'				
	.2	.4	.6	.8	1.0
.01	.22	.37	.52	.60	.65
.02	.12	.21	.30	.37	.43
.03	.08	.14	.20	.27	.33
.04	.04	.11	.16	.20	.29
.05	.03	.09	.13	.16	.20

TABLE IV

Summary of Wien Filter Parameters

	Plane Parallel Plate Filter	Stigmatic Filter
Length (cm)	15	21.2
Entrance Slit (cm)	.15 x 1.00	.15 x 1.00
Exit Slit (cm)	.15 x 2.6	.15 x 1.00
B_o (gauss)	978	978
E_{max} (V/cm)	489	489
$\Delta M/M$	.03	.03
Horizontal Angular Acceptance	±.6°	±5°
Vertical Angular Acceptance	±.6°	±8.5°
M/Z Range	1.5-4.5	1.5-4.5
Solar Wind Velocity Range (km/sec)	300-500	300-500

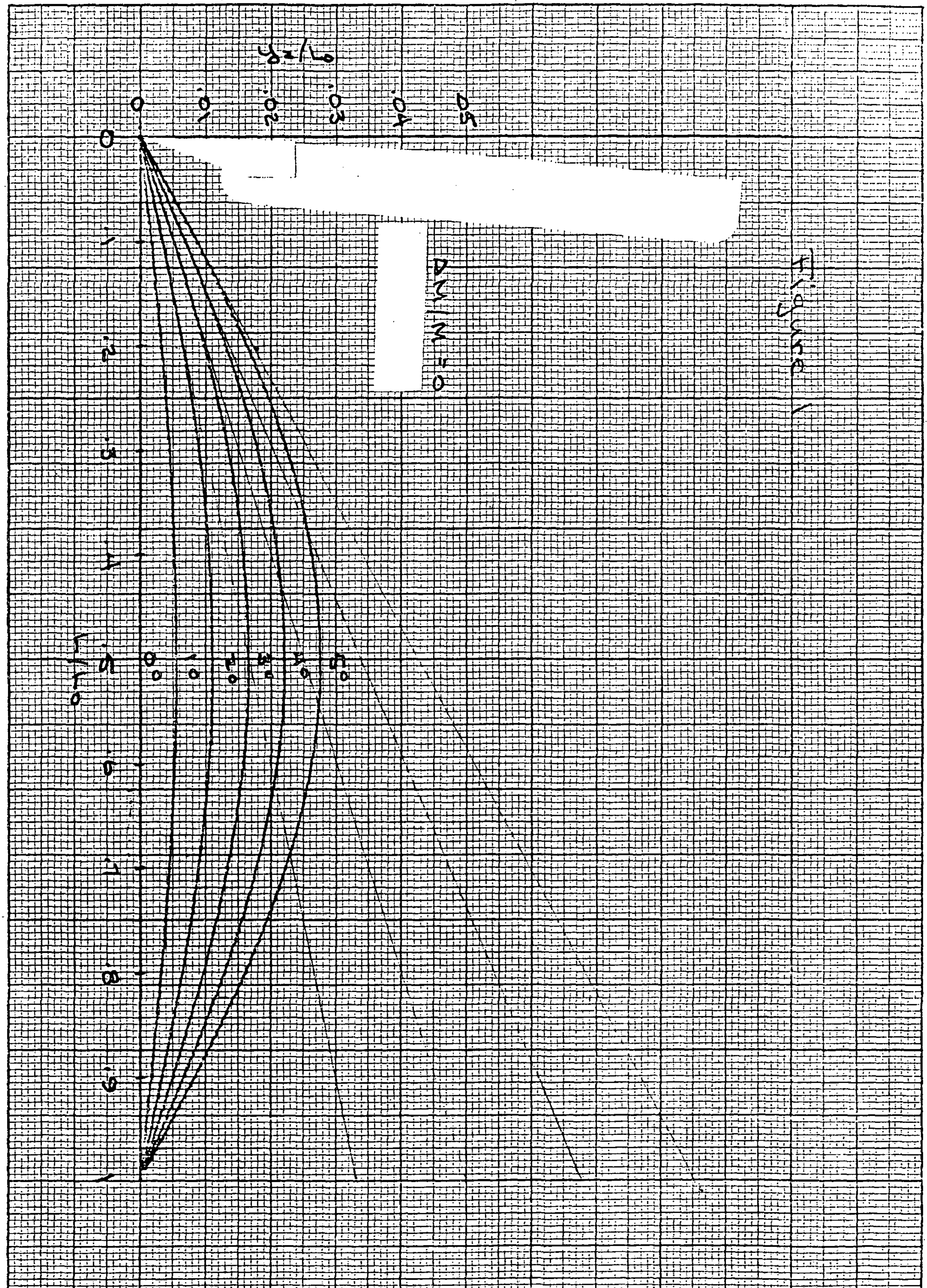
ΔM/M = 0
Figure 1

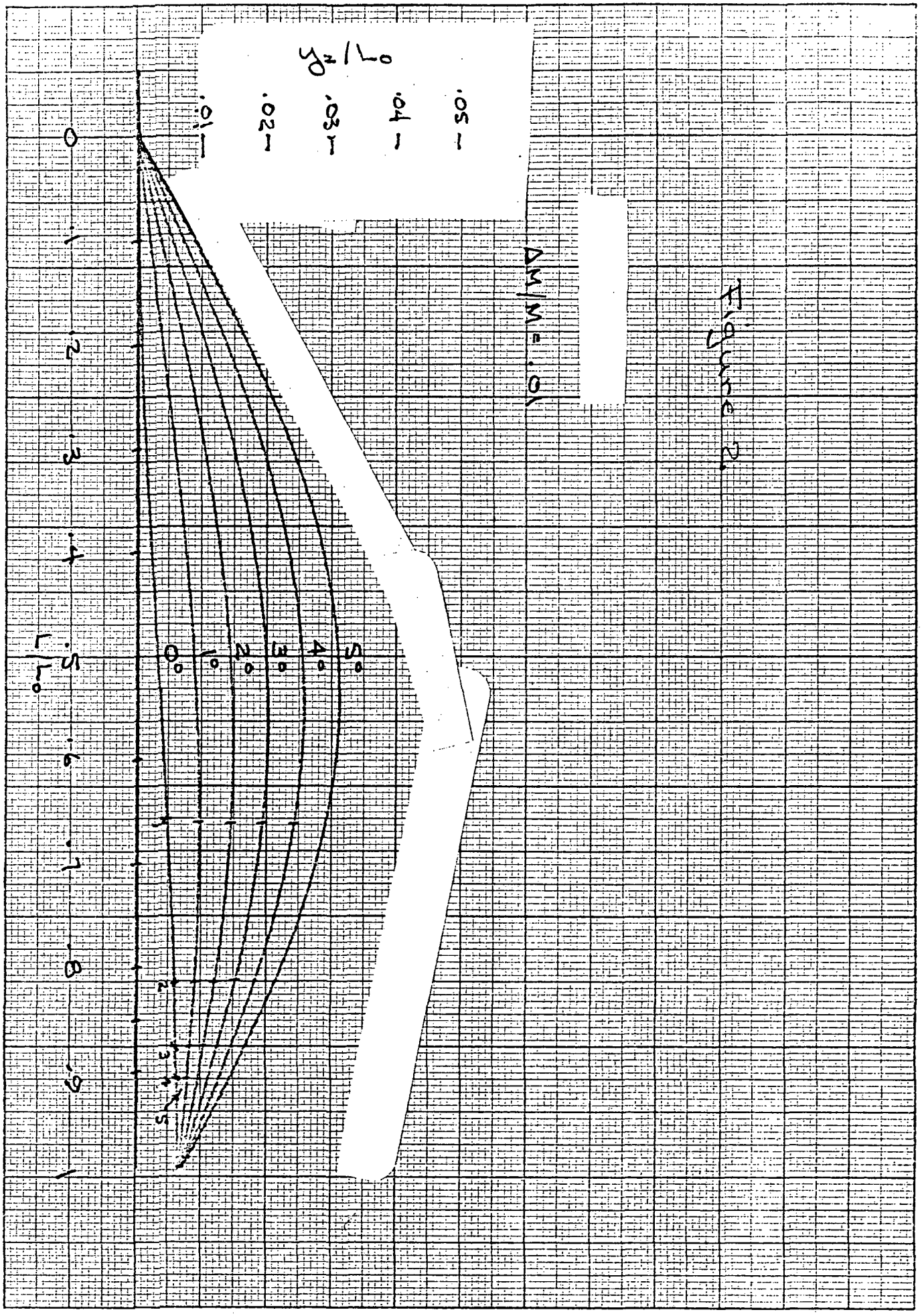
y^2/L_0
.01
.02
.03
.04
.05
$\Delta M/M = .01$
r/r_0
0
.1
.2
.3
.4
.5
.6
.7
.8
.9
0_0
1_0
2_0
3_0
4_0
5_0
1
2
3
4
5

Figure 2.

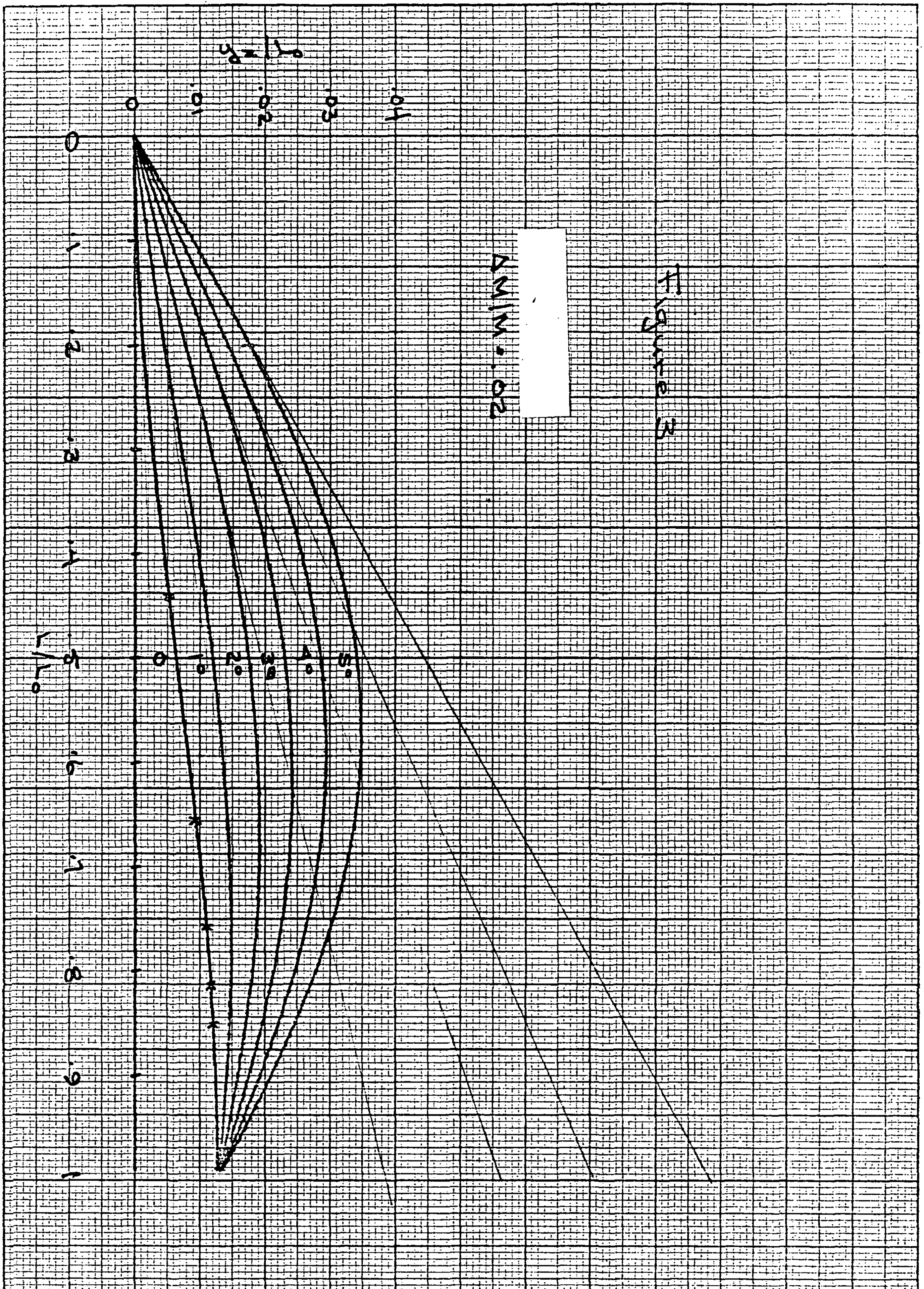
Figure 3
ΔM/M = .02
y/L₀
0
.01
.02
.03
.04
L/L₀
.1
.2
.3
.4
.5
.6
.7
.8
.9
1
0
10
20
30
40
50

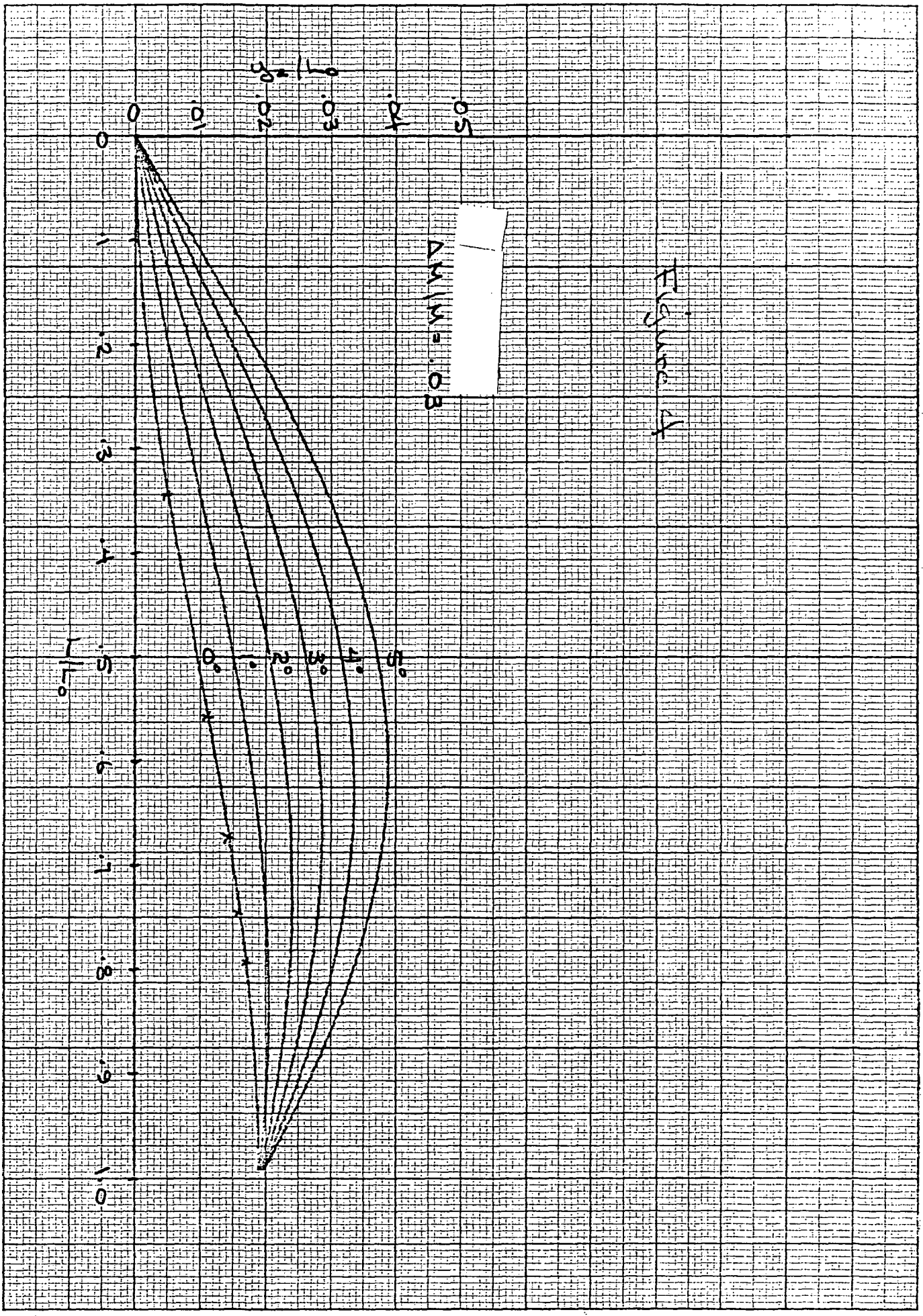
0
0.1
0.2
0.3
0.4
0.5
3b/L0
0
0.1
0.2
0.3
0.4
0.5
0.6
0.7
0.8
0.9
1.0
T/T0
0.0
1.0
2.0
3.0
4.0
5.0
ΔM/M = 0.03

Figure 4

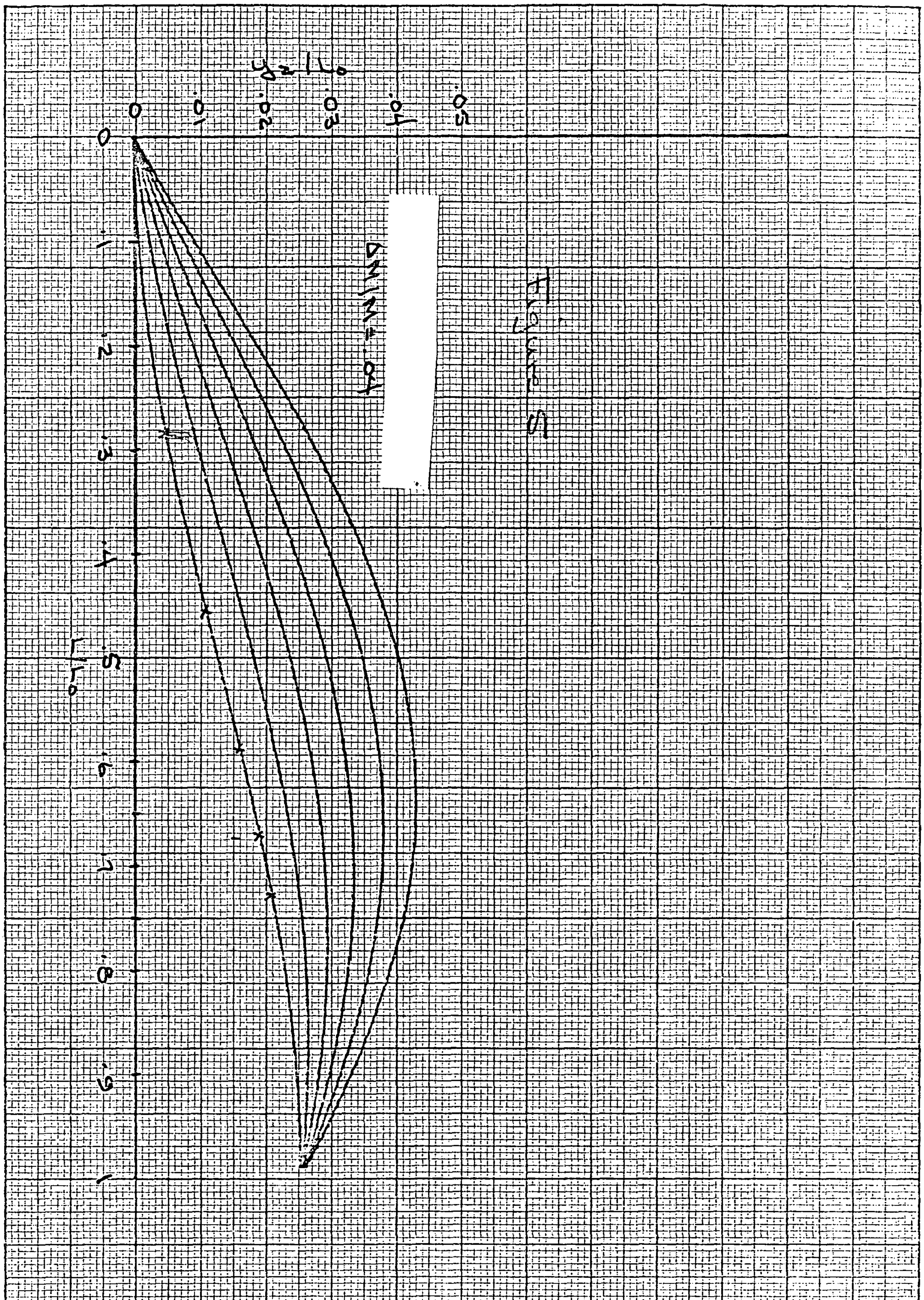
Figure 5
ΔM/M = .04
0 .01 .02 .03 .04 .05
0 .1 .2 .3 .4 .5 .6 .7 .8 .9 1

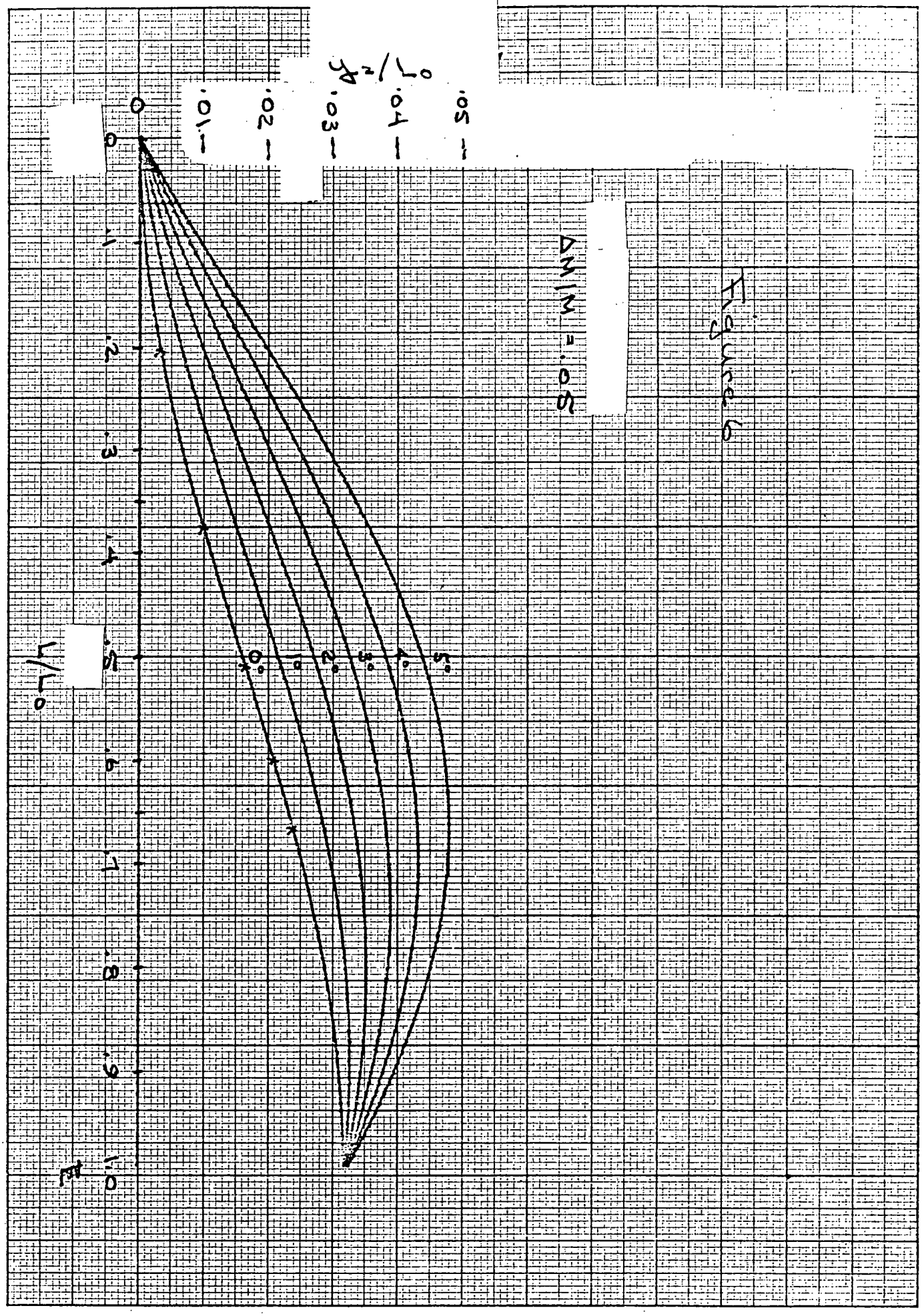
$\Delta M/M = .05$
$\gamma A^2/L_0$
0
.01
.02
.03
.04
.05
h/L_0
0
.1
.2
.3
.4
.5
.6
.7
.8
.9
1.0
0.0
1.0
2.0
3.0
4.0
5.0

Figure 6

Figure 11

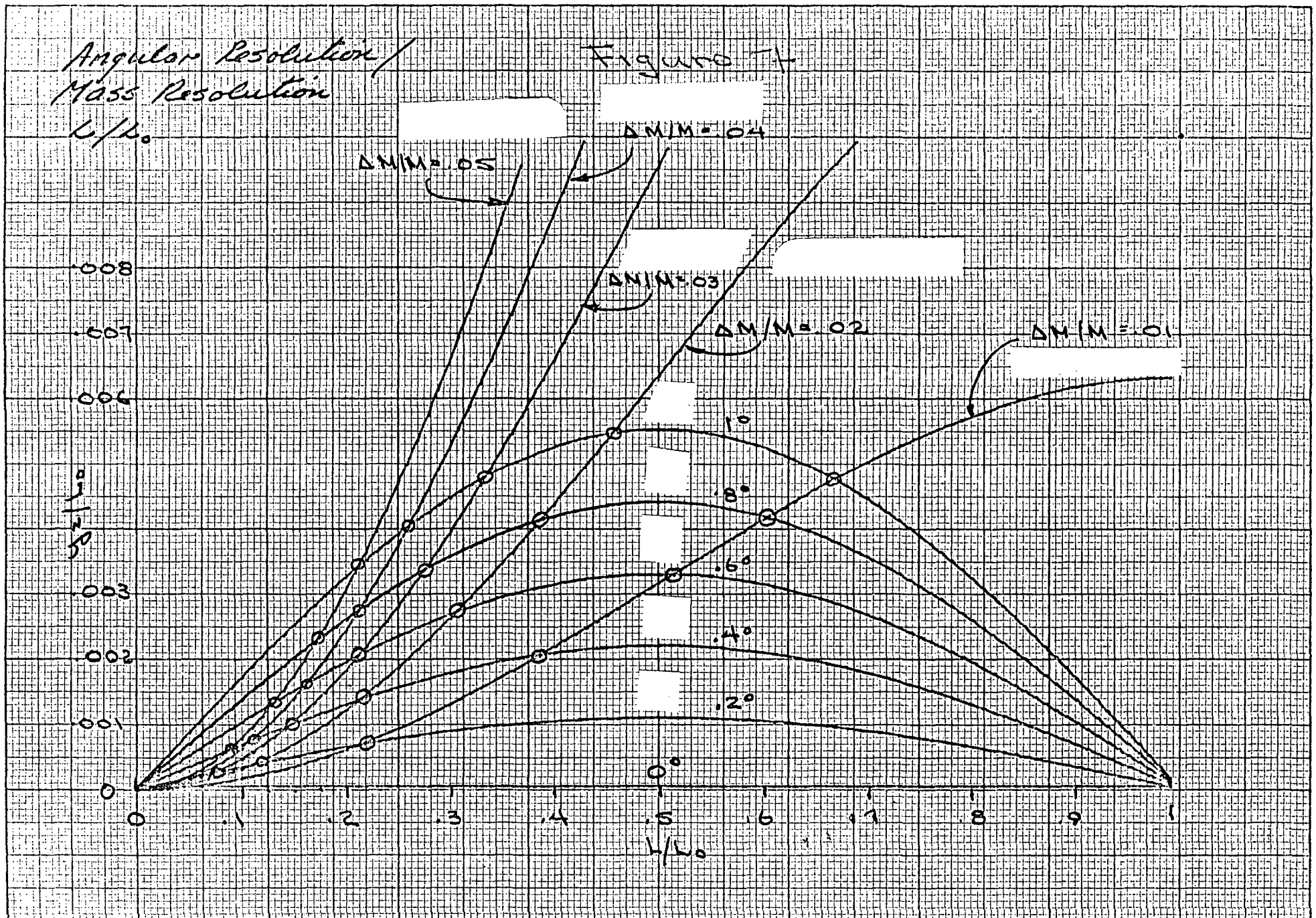
Angular Resolution / Mass Resolution
L/L₀
ΔM/M=.05
ΔM/M=.04
ΔM/M=.03
ΔM/M=.02
ΔM/M=.01
.008
.007
.006
.003
.002
.001
0
Δ1/2θ
10°
.8°
.6°
.4°
.2°
0°
0
.1
.2
.3
.4
.5
.6
.7
.8
.9
1
L/L₀